School of Mechanical Engineering Faculty Publications

School of Mechanical Engineering

2019

Improved Batch Reverse Osmosis Configuration for Better Energy Effiency

Sandra P. Cordoba

Abhimanyu Das

David M. Warsinger

IMPROVED BATCH REVERSE OSMOSIS CONFIGURATION FOR BETTER ENERGY EFFIENCY

IDA 2019 World Congress World Congress on Water Reuse and Desalination, Dubai, UAE, October 20-24, 2019,

Authors: *Sandra P. Córdoba, Abhimanyu Das, David M. Warsinger.*

Presenter: David M. Warsinger, PhD
Assistant professor – Purdue University – United States
david.warsinger@gmail.com

I. ABSTRACT

Recent progress in batch and semi-batch reverse osmosis processes such as CCRO have shown the promise to be the most efficient desalination systems. Despite their progress, it is critical to further increase their efficiencies, and reduce the downtime between cycles that worsens their cost performance. In this study, we model in new detail a further improved batch desalination system that uses a high pressure feed tank with a reciprocating piston. A high-pressure pump fills the inactive side with the following cycle's feedwater, providing two main benefits. First, no tank emptying step is needed because feed is already present, thus reducing downtime. Second, the tank fully empties each cycle, thus avoiding the small energy losses from brine mixing with the new feed that past best designs had. The modeling methodology is the most thorough yet for batch processes, as it uses a discretized module that includes transient mass transport equations for salt boundary layers, membrane permeability effects, and minute salt permeation through the membrane. Comparing the new configuration to standard reverse osmosis with and without energy recovery, the new process vastly outperforms, with the potential to be below 2 kWh/m3 for seawater. The new process has less downtime too, around 2% of cycle time, compared with 10% for CCRO or 16% from past batch studies.

II.   BACKGROUND

Reverse Osmosis (RO) desalination technology was initially developed in the late 1950s, and has now evolved into the leading desalination technology globally [1], accounting for almost 69% of the total installed capacity around the world [2].

Even though the technology has proved its effectiveness and capabilities to treat saline water and take it to required concentration levels for different industries and processes, its elevated energy consumption per every cubic meter of permeate produced is still a main concern.

Figure 1 shows the change in energy consumption for sea water reverse osmosis plants during the last 40 years, although, as better membranes, more efficient pumps and energy recovery devices have been implemented the energy consumption has decayed remarkably we are still far from the least work related with the process.
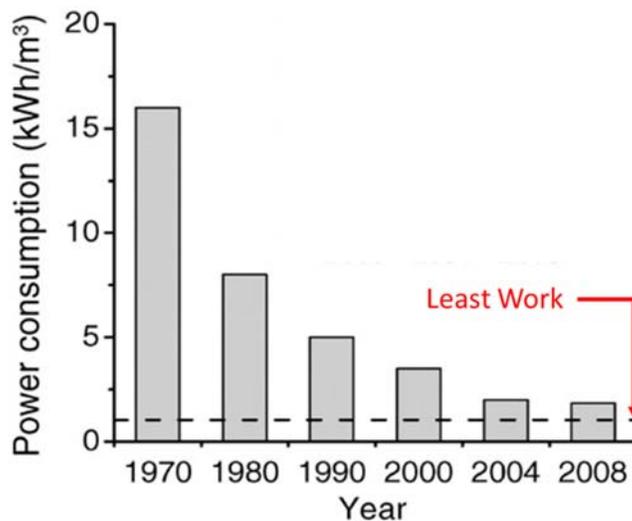

Fig 1. Change in energy consumption in SWRO plants from the 1970s to 2008 - Menachem, E, William A.P. (2011, august 05). [3]

Moreover, most of the desalination plants around the world work under the continuous reverse osmosis configuration in which although the feed osmotic pressure may be relatively low, the entire feed stream must be pressurized to overcome the brine osmotic pressure at the system exit [4].

The term batch refers to a desalination process wherein a set quantity of feed solution is concentrated over time up to the required final brine salinity and this process is repeated to produce large amounts of permeate [5]. Batch RO is a transient process in which the brine exiting the RO module is recirculated back to the feed side without any mixing with fresh feed. The desalination process is extended in time rather than space with a small module recovery ratio per pass. As a result, the exerted hydraulic pressure follows the osmotic pressure of the brine over time leading to significant energy savings as compared to a single stage conventional RO process.

Figure 2 shows the required pressure to be applied in a reverse osmosis plant working under continuous and Batch configuration with an inlet feed salinity of 3 [g/Kg]. In the continuous case, the applied pressure remains constant over time regardless the recovery ratio that has been reached whereas in batch reverse osmosis as the recovery ratio increase and as a consequence the concentration in the inlet feed the applied pressure is augmented. The pink section in the graph can be considered as the energy savings related with using a batch process over a continuous configuration.
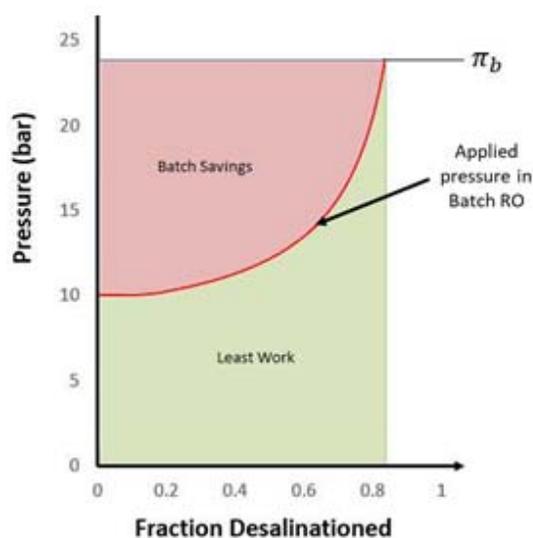

Fig 2. Applied pressure vs RR for continuous and batch RO with feed salinity: 3 [g/kg]

Previously Warsinger et al [6] presented two different configurations to implement batch reverse osmosis. In the first one, a high pressure, variable-volume tank is used to accommodate the exiting brine and the permeate produced in each cycle. In the second one in order to use only existing components an atmospheric pressure tank and a pressure exchanger are used. Nevertheless, the high-pressure tank arrangement presented in this study arose as the most efficient configuration in comparison with continuous and CCRO processes, the practical aspects associated with its implementation limit the real energy consumption that can be achieved [9].

In this study, we developed an improved reverse osmosis configuration to overcome the most important limitations during the practical implementation of the high-pressure tank batch reverse osmosis configuration.

III. RESEARCH CONDUCTED

3.1 Proposed Configuration

A scheme of the proposed configuration for the improved batch reverse process is presented in figure 3. The process is divided in different steps as follows:
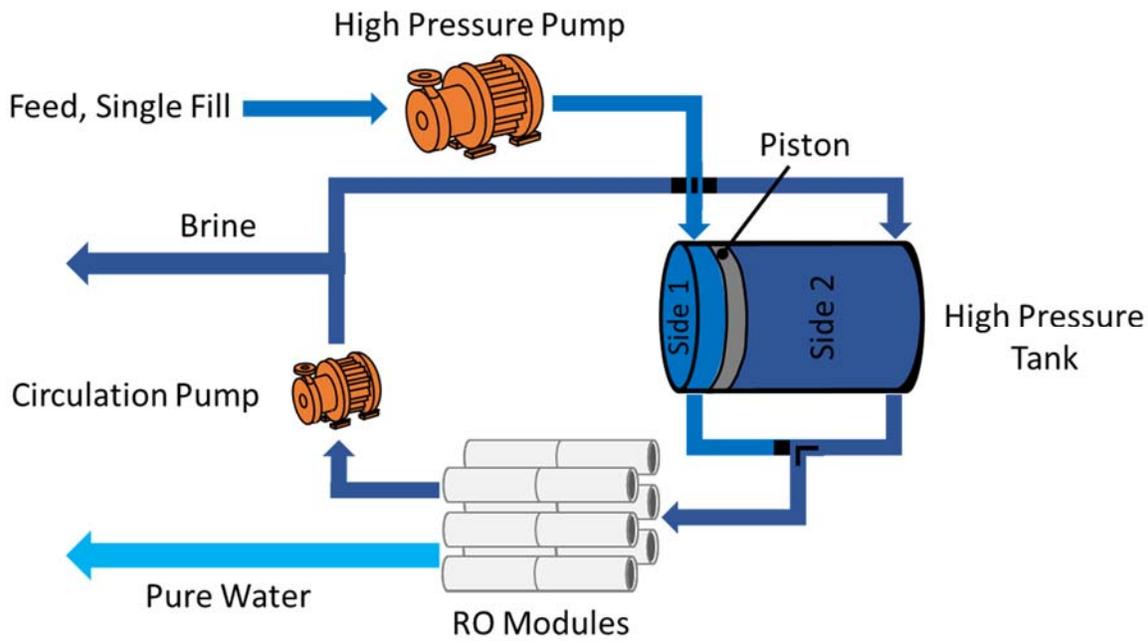

Fig 3. Improved configuration for batch reverse osmosis. Like the original proposed batch process, a high pressure tank enables pressure ramping without losses. Unlike previous designs, both sides of the tank are used for the feed/brine, in an alternating fashion. In batch RO, concentrating feed recirculates in the main flow loop, enabled by a circulation pump with small ΔP. Feed added to the system (through a high-pressure pump that ramps up pressure to follow osmotic pressure) displaces volume on the non-active side, allowing permeate production while maintaining high pressure. Here brine empties at the beginning of each cycle, instead of pausing the cycle for emptying.

Step 0: During the first step of the cycle the high-pressure pump is used to send feed to the side number 1 of the high-pressure tank. This step occurs only one time and is used to initially charge the system with feed.

Step 1: In step number 1, the high-pressure pump will send feed to the side number 2 of the high-pressure tank and this fluid will be used to push the initial feed in the side number 1 through the RO modules. After the split process occurs in the modules the pure water will be collected in a different location and the produced brine will be returned to the side number 1 of the high-pressure tank using the circulation pump.

Step 2: The moment when the piston reaches the end of the high-pressure tank is the signal to finish step 1 and a quick flushing stage is initiated. A valve closes the recirculation loop, and the circulation pump empties the brine in the pipes and replaces it with feed. Meanwhile, the high-pressure pump will be continue to send feed to the RO modules, produces permeate in a pulse-flow like configuration. Then the

module empties into the flow loop at high pressure, where valves again reduce the pressure to replace the brine with feed. After this stage the system is ready to enter in a water production phase again using the feed in the side number 1 of the high-pressure tank.
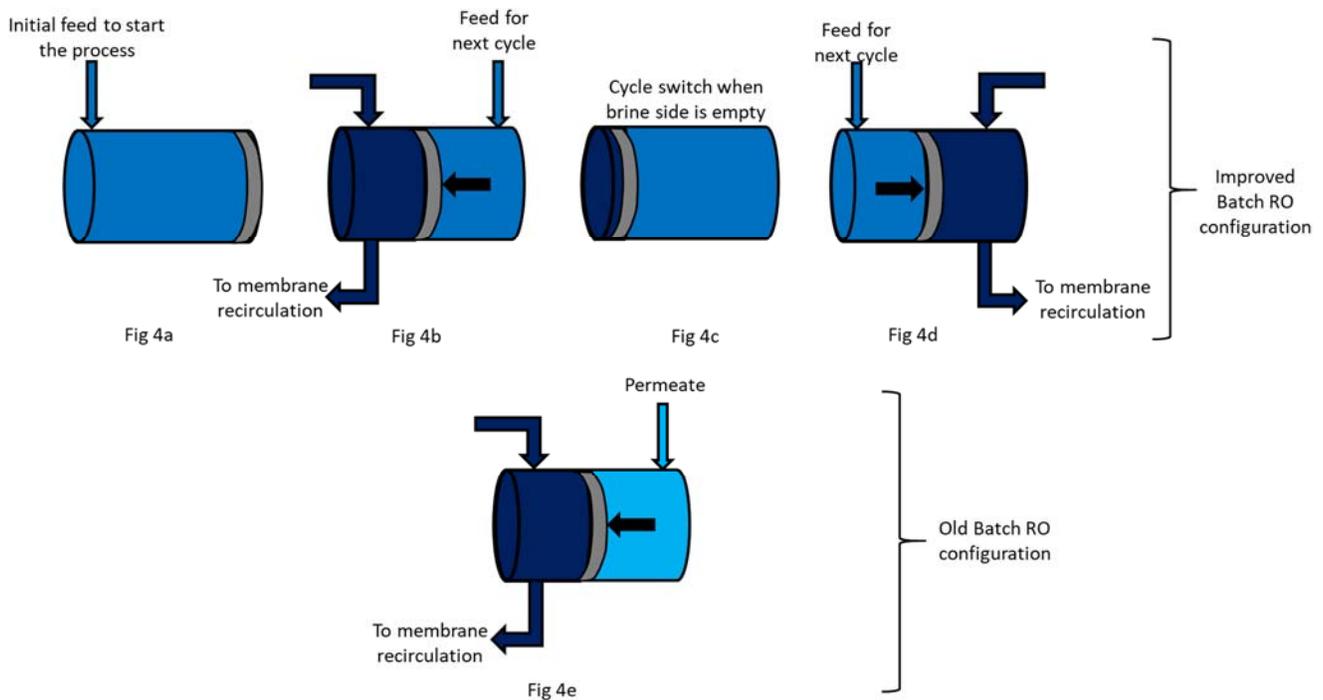

Fig 4. Steps is the improved batch RO configuration vs the old batch RO configuration. The new configuration uses feed/brine on both sides of the piston instead of displacing with permeate as a working fluid.

In figure 4 the different steps for the improved batch RO configuration are shown. Fig 4a corresponds with the step number 1 (filling), figure 4b corresponds with step number 2 (water production using the side number 1 in the high-pressure tank) and figures 3 and 4 represents the cycle switching after flushing out the system to produce permeate using the other side of the high-pressure tank.

Figure 4e represents how the high-pressure tank was being used in the old Batch RO design [6]. Instead of using both sides to produce fresh water, one side was being filled by the permeate causing contamination issues with the fresh water and the brine. Moreover, the downtime in the system during the flushing step is higher because the system needs to be recharged again, unlike the new configuration where these concerns were solved.

Next, some advantages of the new and improved Batch RO configuration over the previous was are discussed:

- As mentioned before, the downtime caused by the flushing step is reduced substantially, because now, only the leftover brine in the pipes and in the module needs to be removed and on the other hand, it is not necessary to recharge the system as the feed send to the opposite side of the high pressure tank is used in the next step to produce permeate water.

- The entropy generation in this improved configuration is reduced in comparison with the previous design as mixing between the incoming feed and the remaining brine in the system is avoided. This occurs because no brine remains in the tank when a cycle is ended.

- Regarding practical aspects for the implementation of the Batch RO process, in the previous design, as the mechanical seal in the piston is not perfect, there was a possibility of contaminating the permeate water produced with the brine in the other side of the tank. In the new configuration this problem is solved because the permeate will not be in contact neither with the initial feed or the brine.

3.2 Modeling Process

In this study, we solve the transient mass conservation and transport equations for the Batch RO processes while breaking up the RO module into many discretized slices, to account for the concentration boundary and flux in effectively 2D detail. To accurately estimate energy efficiency, realistic pump efficiencies are used for the high-pressure pump as well as the circulation pump and realistic pressure drops are calculated. The temporal and spatial variation of salinity in the feed and permeate channels are captured by solving the unsteady mass conservation equations for both water and salt. Unsteady concentration polarization effects have also been captured by solving the transient transport equation for flow across the membrane. Boundary layer thickness on either side of the membrane is obtained by using mass transfer correlations that can incorporate the effect spacers in the channels. Pressure drop in the flow channels is obtained using Darcy's law that depends on the Reynolds number of the flow. Local density variations with salinity have also been modelled and included in the conservation equations.

In the following section the modeling procedure adopted is commented in detail. The discretized control volume used in the numerical simulation for Batch RO is described and the equations to calculate transmembrane water and salt flux are shown. Moreover, the transient transport equation governing the convection-diffusion is presented along with the transient mass conservation equations for water and salt.

During the simulation, the subscript i was used to denote the ith discretized control volume, as shown in figure 5, along the longitudinal flow direction with respect to the membrane and assuming a salinity invariant membrane permeability coefficient, A, the transmembrane water flux for the can be written as:

$$J_{w,i} = A(\Delta P_i - \Delta \pi_i) \qquad (1)$$

where ΔP_i and $\Delta \pi_i$ are respectively the hydraulic and osmotic pressure differences across the RO membrane. The osmotic pressure difference, $\Delta \pi_i$, across the membrane depends on the salt concentration difference across the active layer of the membrane and is given by
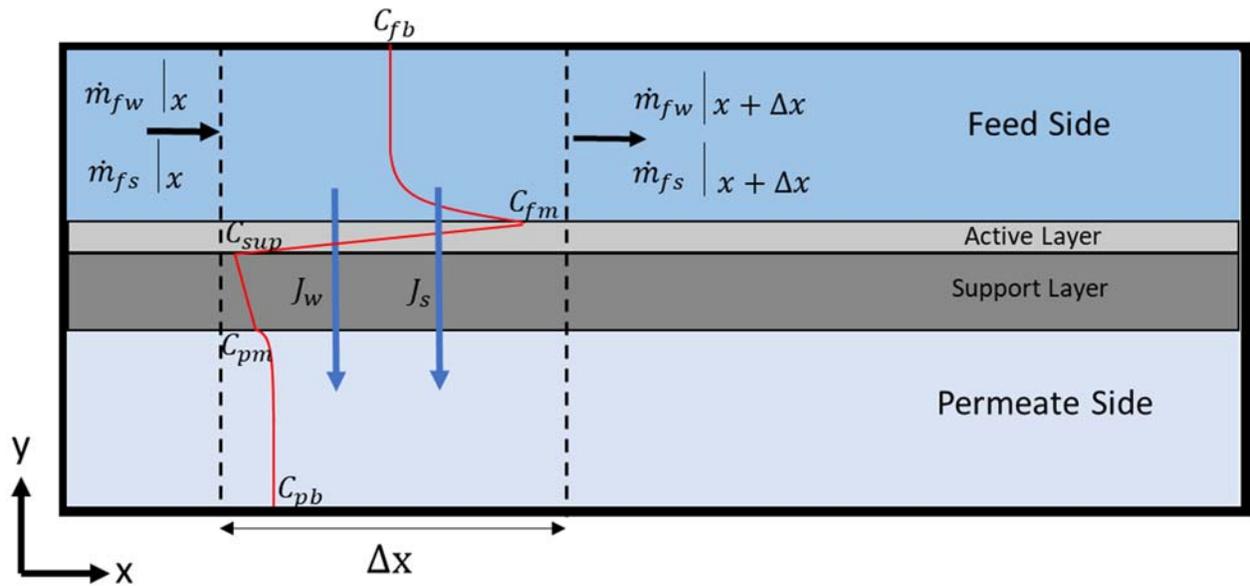
Fig 5. Discretize control volume used in the numerical simulation for Batch RO

$$\Delta C_{m,i} = C_{fm,i} - C_{sup,i} \qquad (2)$$

where $C_{m,i}$ is the salt concentration at the membrane surface on the feed side of the RO module, while $C_{sup,i}$ is the salt concentration at the interface between the active layer and the support layer.

The value of $C_{fm,i}$ is higher than the bulk value of salt concentration on the feed side, $C_{fb,i}$ while that of $C_{sup,i}$ is lower than bulk value on the permeate side, $C_{pb,i}$. The values of $C_{fm,i}$ and $C_{sup,i}$ depend on the bulk concentration values, the thickness, tortuosity and porosity of the membrane support layer and the flow velocity over the membrane surface dictating the concentration boundary layer thickness on either side of the membrane as well as the water flux, $J_{w,i}$. $\Delta C_{m,i}$ can be calculated by solving the transient transport equation for different domains along the transmembrane direction, y which be written as:

$$\frac{\partial C_i(y)}{\partial t} + J_w \frac{\partial C_i(y)}{\partial y} = D \frac{\partial^2 C_i(y)}{\partial y^2} \qquad (3)$$

where, $C_i(y)$ is the transmembrane salt concentration, y and D is the binary diffusion coefficient of salt in water. In solving (3), we ignore the small temporal and spatial variation of density as well as water flux across the membrane to reduce the complexity of the model. The boundary conditions for (3) depend on the transmembrane salt flux, $J_{s,i}$. Most membranes do not have a 100% salt rejection rate and hence the permeate should be expected to have a small salinity owing due to $J_{s,i}$. Moreover, if we assume a constant salt permeability coefficient, B, for a membrane, $J_{s,i}$, the transmembrane salt flux, may be written as

$$J_{s,i} = B\Delta C_{m,i} \qquad (4)$$

Bulk values of salt concentration in the feed and permeate channels of the module can be obtained by solving the transient mass conservation equations for water and salt for control volumes on either side of the membrane which can be written as

$$A_f \Delta x \frac{\partial \rho_{f,avg,i}(1-C_{f,avg,i})}{\partial t} = m_{f,w,i} - m_{f,w,i+1} - J_{w,i}\Delta A \rho_w \qquad (5)$$

$$A_f \Delta x \frac{\partial \rho_{f,avg,i}C_{f,avg,i}}{\partial t} = \frac{m_{f,w,i}C_{f,i}}{1-C_{f,i}} - \frac{m_{f,w,i+1}C_{f,i+1}}{1-C_{f,i+1}} - J_{s,i}\Delta A \rho_s \qquad (6)$$

where the subscript f denotes the feed side, A_f is the channel cross-sectional flow area, Δx is the length of each control volume, and $\rho_{f,avg,i}$ and $C_{f,avg,i}$ are the average bulk solution density and concentration in the control volume. $m_{f,w,i}$ and $C_{f,i}$, and $m_{f,w,i+1}$ and $C_{f,i+1}$ are the water flow rate and bulk concentration of the steams entering and leaving the ith control volume, while $J_{w,i}$ and $J_{s,i}$ are the water and salt fluxes leaving the same control volume. ΔA is the differential membrane area for transmembrane transport while ρ_w and ρ_s are the densities of water and salt. Similar equations can be constructed for flow on the permeate side as well with the salt and water fluxes entering the control volume.

IV.   RESULTS

In figure 6 the specific energy consumption of the batch RO, continuous reverse osmosis and continuous reverse osmosis with a pressure exchanger was plotted for a wide range of initial concentrations and final RR. It can be observed how the batch RO configuration remarkably outperforms the performance of its competitors having very low specific energy consumptions compared with the other arrangements under the same initial conditions.
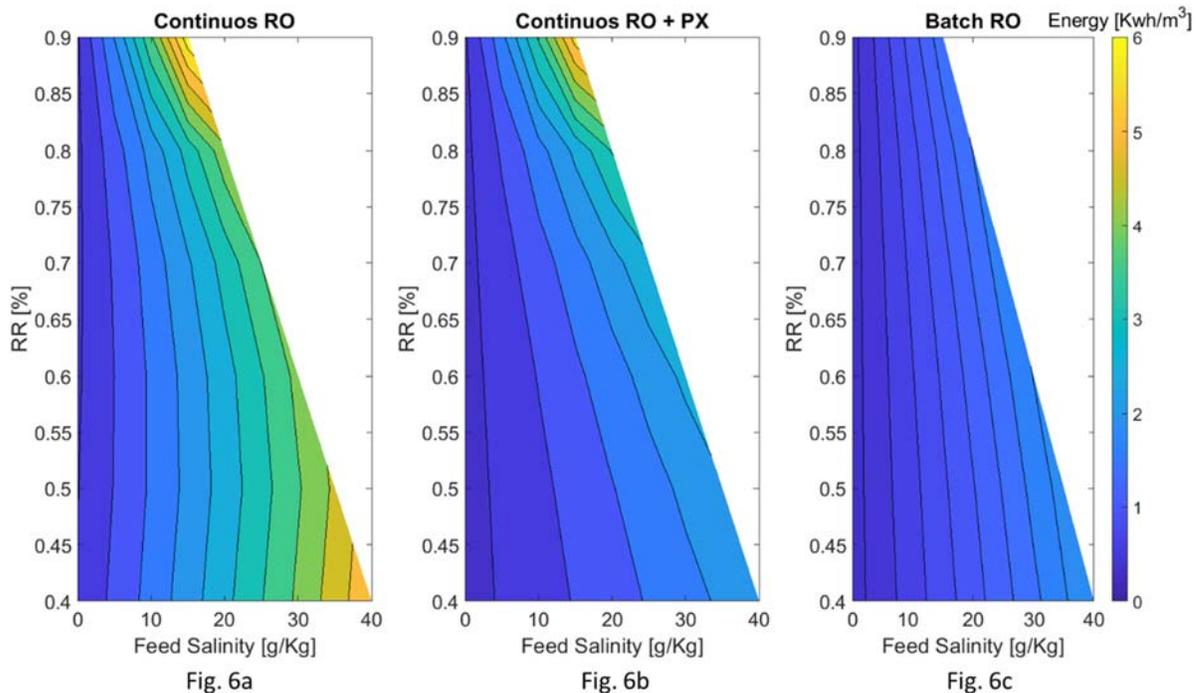

Fig. 6a   Fig. 6b   Fig. 6c

Fig 6. A map of Specific Energy consumption by inlet feed salinity for the leading two RO configurations (continuous RO, continuous RO + PX (a pressure recovery device)), and the new batch configuration.

In figure 7 the downtime percentage for different Batch or Semi-Batch RO configurations with respect to the total cycle time is shown.

The downtime in Close Circuit Reverse Osmosis processes was taken from data information given by Desalitech for their CCRO set ups [8], the downtime for the old batch configuration was taken from information presented in the experimental work conducted in [4] and finally the downtime for the new batch RO configuration was calculated for system with initial feed with a concentration of 35 [g/Kg] and a recovery ratio of 50%. It can be seen how the downtime in the new configuration smaller compared with the time spent in the flushing step in the old configuration. The new design in its simplest operation can achieve 10% downtime, but with steps to use valves to replace the feed and module water, can get far lower.
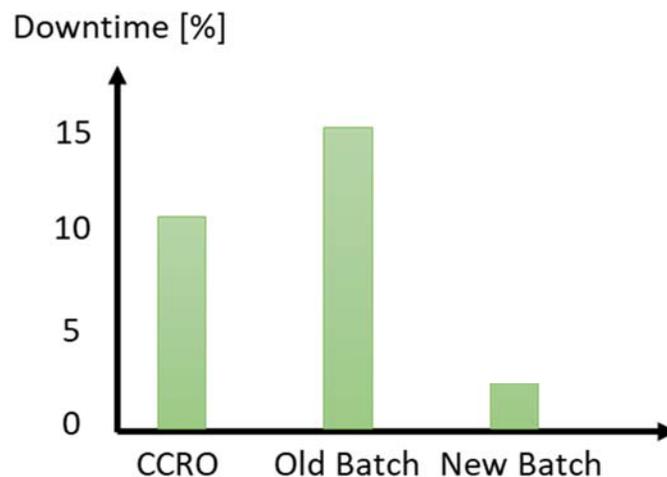

Fig 7. Downtime percentage for Close Circuit Reverse Osmosis (CCRO) and the two Batch RO configurations studied, with respect to the total cycle time.

V.   CONCLUSIONS

This work showed how the Batch RO process can be pushed one step further by using an improved design which allows the technology to overcome some of the factors that may reduce the efficiency in the system.

Two primary conclusions were found:

- The downtown in the new and improved configuration due to the flushing step can be reduce substantially in comparison with the previous configuration, because, on the one hand only the leftover brine in the pipes and the modules must be removed and moreover no feeding steps are needed at the beginning of each cycle because the feed sent to one the sides of the high-pressure tank is used as working fluid for the new cycle.

- A far more detailed model of Batch RO, using transient concentration polarization and a realistic membrane confirms the anticipated superior efficiency.

VI.   REFERENCES

1.   IDE Technologies. What is desalination? Retrieve from:
      https://www.idetech.com/en/solutions/desalination/what-is-desalination/
2.   Jones, E., Qadir, M., Vliet, M., Smakhtin, V., MuKang, S. The state of desalination and brine
      production: A global outlook. Science of the Total Environment 657 (2019), 1343-1356.
3.   Elimelech, M., Phillip, W.A. The Future of Seawater Desalination: Energy, Technology, and the
      Environment. Science 333 (2011), 712-717.
4.   Wei, Quantum J. et al. Batch reverse osmosis: experimental results, model validation and design
      implications. 2019 AMTA/AWWA Membrane Technology Conference & Exposition.
5.   Warsinger, D.M., Tow, E.W., Maswadeth, L.A., Connors, G.B., Jaichander, S., Lienhard J.V.
      Inorganic fouling mitigation by salinity cycling in batch reverse Osmosis. Water Research 137
      (2018), 384-394.
6.   Warsinger, D.M., Tow, E.W., Nayar, K.G., Maswadeth, L.A., Lienhard J.V. Energy effieicmcy of
      batch and semi-batch (CCRO) reverse osmosis desalination. Water Research 106 (2016), 272-282.
7.   Bouma, A.T., Lienhard J.V. Split-feed counterflow reverse osmosis for brine concentration.
      Desalination 445 (2018), 280-291.
8.   Efraty A. (2019). Desalitech's Advanced "Super RO" Technologies of the 21st Century
9.   Swaminathan J., Lienhard J.V. Practical aspects of Batch RO design for energy-efficient seawater
      desalination. Desalination 470 (2019). 114097

VII.   ACKNOWLEDGEMENT